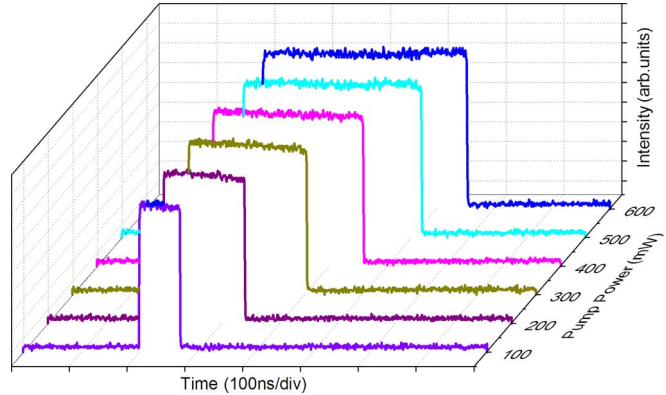


Observation of Dissipative Soliton Resonance in a Net-Normal Dispersion Figure-of-Eight Fiber Laser

Volume 5, Number 3, June 2013

Jin-hui Yang
Chun-yu Guo
Shuang-chen Ruan
De-qin Ouyang
Huai-qin Lin
Yi-ming Wu
Ru-hua Wen



DOI: 10.1109/JPHOT.2013.2265982
1943-0655/\$31.00 ©2013 IEEE

Observation of Dissipative Soliton Resonance in a Net-Normal Dispersion Figure-of-Eight Fiber Laser

Jin-hui Yang, Chun-yu Guo, Shuang-chen Ruan, De-qin Ouyang,
Huai-qin Lin, Yi-ming Wu, and Ru-hua Wen

Shenzhen Key Laboratory of Laser Engineering, Key Laboratory of Advanced Optical Precision Manufacturing Technology of Guangdong Higher Education Institutes, College of Electronic Science and Technology, Shenzhen University, Shenzhen 518060, China

DOI: 10.1109/JPHOT.2013.2265982
1943-0655/\$31.00 ©2013 IEEE

Manuscript received April 23, 2013; revised May 22, 2013; accepted May 24, 2013. Date of publication May 31, 2013; date of current version June 11, 2013. This work was supported in part by the NSFC under Grant 61275144, by the Doctoral Program of High School Research Fund under Grant 20104408110002, by the Key Program of Basic Research Project of Shenzhen under Grant JC201005250048A, by the Improvement and Development Project of Shenzhen Key Lab under Grant CXB201005240014A, and by the Natural Science Foundation of SZU under Grant 201203. Corresponding authors: C.-Y. Guo and S.-C. Ruan (e-mail: cyguo@szu.edu.cn; scruan@szu.edu.cn).

Abstract: High-energy square pulses operating in dissipative soliton resonance region are experimentally observed in an erbium-doped figure-of-eight fiber laser with large net-normal dispersion for the first time to our knowledge. The dissipative soliton resonance is achieved by using the nonlinear-amplifying-loop-mirror mode-locked technique. The output pulse duration broadens linearly with the increase of pump power, while the peak power maintains a constant value. At the maximum pump power of 620 mW, the intracavity pulse energy is up to 379.2 nJ, and the average output power is 14.02 mW.

Index Terms: Fiber lasers, mode-locked lasers, solitons.

1. Introduction

Passively mode-locked fiber lasers, as ideal ultrashort pulse optical sources, have attracted significant interest for their wide applications. Particularly, the ultrashort pulse laser with high-energy is required in such diverse fields as micromachining, material processing, and supercontinuum generation. During the past decades, lots of research concentrated on the generation of high-energy ultrashort mode-locked pulses directly from an oscillator. Different types of fiber lasers have been proposed to generate high-energy mode-locked pulses, such as stretched-pulse fiber lasers [1]–[3], self-similar fiber lasers [4], [5], and all-normal-dispersion (ANDi) fiber lasers [6]–[8]. However, wave breaking or multipulse generally occurs in the laser cavity mainly due to the overdriven nonlinear effect under strong pump power, which restricts further scaling of pulse energy.

In recent years, high-energy nanosecond square pulses without wave breaking generated from passively mode-locked fiber lasers have also been investigated intensively [9], [10]. Square pulse emission from a passively mode-locked erbium-doped fiber (EDF) laser was first observed in a figure-of-eight cavity based on nonlinear amplifying loop mirror (NALM) mode-locked technique [11]. In 2007, Schmieder *et al.* also reported the square-pulse generation from figure-of-eight laser with a highly nonlinear dispersion shifted fiber [12]. Furthermore, the nonlinear polarization rotation (NPR) mode-locked technique has also been applied to generate square pulses. Matsas *et al.* first demonstrated the generation of square pulses in a passively mode-locked fiber ring laser [13].

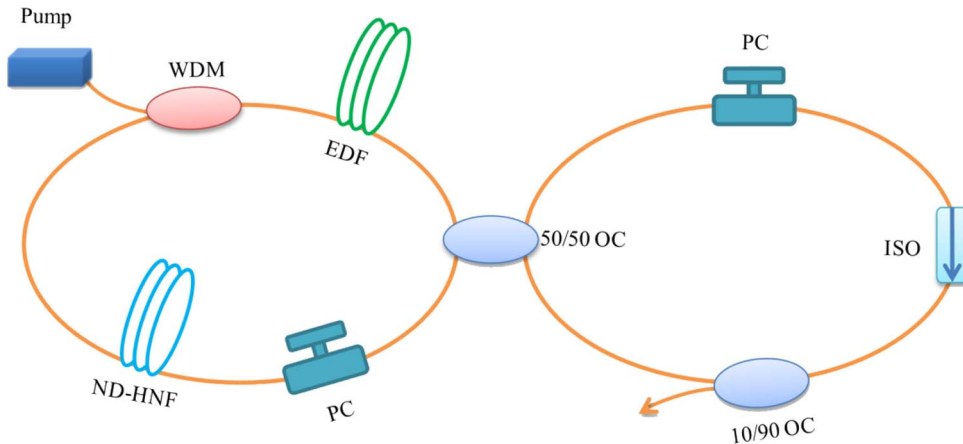


Fig. 1. Experimental setup of the figure-of-eight fiber laser. EDF: erbium doped fiber; WDM: wavelength division multiplexer; ND-HNF: normal-dispersion high-nonlinearity fiber; PC: polarization controller; OC: optical coupler; ISO: isolator.

However, the aforementioned reports only focused on square-pulse generation but did not give the mechanism. Moreover, the pulse energy of the laser had not been considered.

Recently, a new concept, namely, the dissipative soliton resonance (DSR), has been proposed to increase the pulse energy from a fiber laser [14]–[16]. The formation of dissipative solitons, which requires a balance between the gain and the loss, is governed by the cubic–quintic Ginzburg–Landau equation (CGLE) [14], [15]. For particular parameters, the pulse energy can be enhanced to a large value without pulse breakup, and the pulse duration increases linearly with pump power [15]. In addition, the pulse shapes have a square profile at certain values of system parameters [17], [18]. By using NALM mode-locked technique, the square pulses operating in DSR region have been experimentally investigated in fiber ring lasers with normal dispersion [19] and anomalous dispersion [20]. The square-pulse DSR generation has also been reported in figure-of-eight laser operating in anomalous dispersion regime, but the pulse energy is limited to 3.25 nJ [21]. The pulse energy in figure-of-eight laser can further be improved by selecting appropriate parameters. Generally, the fiber lasers operating in normal dispersion regime allow higher pulse energy [8], [22], [23]. However, to the best of our knowledge, there is no report about square-pulse DSR generation in the normal-dispersion figure-of-eight fiber laser, and the investigation would be beneficial to understand the DSR generation in figure-of-eight lasers comprehensively.

In this paper, the high-energy square-pulse DSR is experimentally observed in an erbium-doped figure-of-eight fiber laser with large net-normal dispersion by using NALM mode-locked technique. Stable pulses with a repetition rate of 369.7 kHz are obtained. With the increase of pump power, the duration of the square pulse increases linearly from 23.9 ns to 363.9 ns, while the peak power maintains a constant value. Moreover, the intracavity pulse energy reaches up to 379.2 nJ without wave breaking.

2. Experimental Setup

The experimental configuration of the figure-of-eight laser with large net-normal dispersion is shown schematically in Fig. 1. The NALM, which acts as a fast saturable absorber [3], is depicted on the left-hand side. The fiber loop on the right-hand side is a unidirectional ring (UR) cavity, which is connected to the NALM by a 3-dB coupler. The NALM consists of a 980/1550-nm wavelength division multiplexer (WDM), a polarization controller (PC), a 19.5-m EDF and a normal-dispersion high-nonlinearity fiber (ND-HNF) with the length of 520 m. The UR cavity includes a PC, an isolator (ISO) and a 10/90 fused optical coupler (OC). The EDF with the group velocity dispersion (GVD) parameter of -12.2 ps/nm/km and an absorption coefficient of 7 dB/m at 980 nm is pumped by a

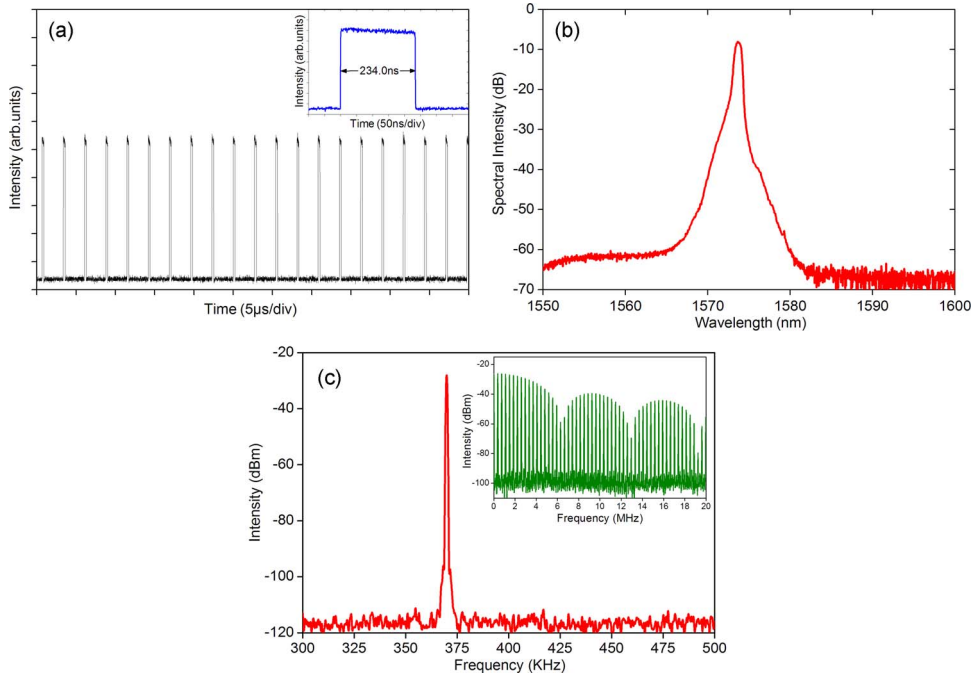


Fig. 2. Typical square-pulse emission. (a) Oscilloscope trace of the square pulse. Inset: a single square pulse. (b) Corresponding optical spectrum. (c) RF spectrum of the output pulse. Inset: wideband RF spectrum up to 20 MHz.

976-nm single-mode laser diode (LD). The maximum pump power, which can be coupled into the laser, is approximately 620 mW. The ND-HNF with the GVD of -5 ps/nm/km and the nonlinear coefficient of 10 /W/km is introduced into the NALM cavity to increase the nonlinearity. The pigtailed fibers of optical components in the cavity are standard single-mode fibers (SMFs) with the GVD of 17 ps/nm/km , and the total length is 4 m. The cavity length and net cavity dispersion at 1550 nm are 543.5 m and 3.53 ps^2 , respectively. Two PCs are used to control the polarization states of the pulses in the cavity. The ISO enforces the unidirectional operation with the isolation more than 30 dB. An OC with the 10% port as the output port is placed after the ISO. An optical spectrum analyzer (OSA; YOKOGAWA AQ6370B) and a 1-GHz digital phosphor oscilloscope (Tektronix DPO7014C) together with a 45-GHz photoelectric detector (New Focus 1014) are simultaneously employed to monitor the laser spectrum and the output pulse train.

3. Experimental Results and Discussions

The NALM, which is based on the nonlinear phase shift induced by self-phase modulation (SPM) and cross-phase modulation (XPM) [24], [25], was utilized to achieve the self-started passively mode-locked state. In our experiment, the mode-locked threshold is 40 mW. By adjusting the PCs in an appropriate position and setting pressure properly, a train of stable mode-locked square pulses can be obtained when the pump power exceeds the threshold. The typical oscilloscope trace of the pulse output from the fiber laser under the pump power of 350 mW is shown in Fig. 2(a). The mode-locked pulse train has a uniform pulse interval of about $2.7 \mu\text{s}$, corresponding to the cavity roundtrip time, which is determined by the cavity length. As exhibited in the inset in Fig. 2(a), the output pulse has a square profile without other fine internal structure, and the measured pulse duration is 234.0 ns. The corresponding optical spectrum of the square pulse is shown in Fig. 2(b), depicting that the spectrum has a central wavelength of 1573.7 nm and a 3-dB bandwidth of 0.88 nm. The radio frequency (RF) spectrum of the output pulse was measured by a RF spectrum analyzer (Tektronix RSA 3303B), as shown in Fig. 2(c). The fundamental frequency peak is located at

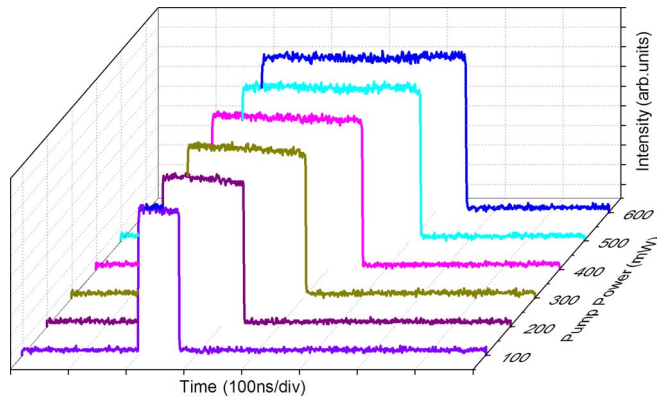


Fig. 3. Square pulses under different pump powers.

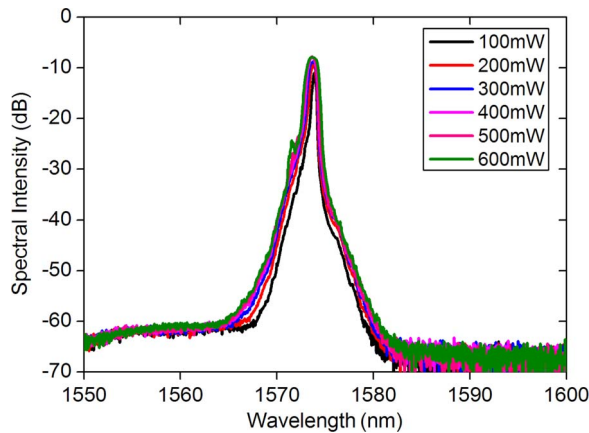


Fig. 4. Optical spectra of the square pulses under different pump powers.

369.7 kHz, and the signal-to-noise ratio (SNR) is larger than 80 dB. The inset in Fig. 2(c) shows the wideband RF spectrum up to 20 MHz, which demonstrates that the fiber laser operates at a stable mode-locked state.

The evolution of square pulse has also been further investigated experimentally. By fixing the PCs, the duration of square pulse can be tuned by changing the pump power. The dynamic of square-pulse broadening with respect to pump power is shown in Fig. 3. The pump powers are selected as 100 mW, 200 mW, 300 mW, 400 mW, 500 mW, and 600 mW here. The corresponding pulse durations are 70.9 ns, 140.7 ns, 204.8 ns, 260.1 ns, 308.3 ns, and 354.4 ns, respectively. As shown in Fig. 3, the output pulse duration broadens with the increase of pump power. However, the pulse amplitude keeps invariable during the process of square-pulse broadening. Moreover, no pulse bunch was observed. The phenomena are different from the nanosecond noiselike pulse, which contains pulse bunch [13]. The corresponding evolution of the optical spectrum exhibits that the spectral intensities and the 3 dB bandwidths of the optical spectra increase slightly, as presented in Fig. 4.

To better show the observed pulse characteristics, Fig. 5(a) exhibits the variations of square-pulse duration and output power with respect to the pump power. As can be seen, both of them monotonically increase with the pump power. At the threshold, the narrowest stable square pulse is 23.9 ns, while the maximum pulse duration is 363.9 ns at the maximum pump power of 620 mW. It should be pointed out that the pulse still has a square profile and is stable at the maximum pump power. Thus, we believe that wider pulses could be obtained with higher pump power. An

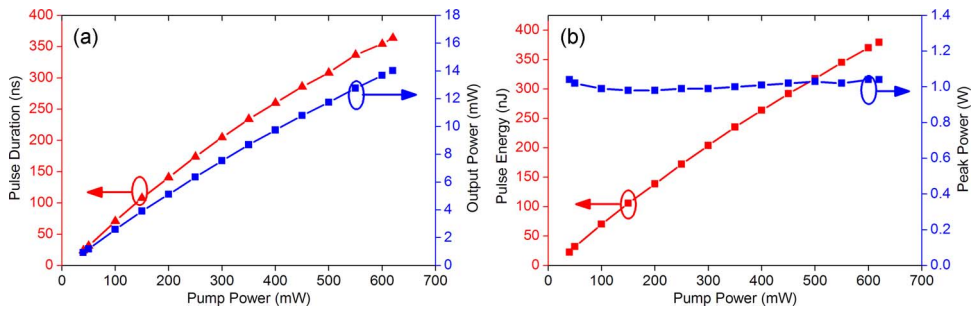


Fig. 5. (a) Pulse durations and output powers versus the pump powers. (b) Pulse energies and peak powers versus pump powers.

extraordinary feature of the square pulse is that the pulse energy could approach a high value without suffering pulse breakup and pulse shape distortion. In our experiment, the largest output power is 14.02 mW at the pump power of 620 mW. Therefore, the output pulse energy is 37.92 nJ. Considering that 10% port of the OC is used as output port, the intracavity pulse energy of the fiber laser is as large as 379.2 nJ. Moreover, no output power saturation phenomenon was observed. Fig. 5(b) exhibits the pulse energy and pulse peak power as a function of the pump power. The pulse energy almost linearly increases with the pump power, while the peak power of the square pulse almost keeps constant inside the cavity. In our experiment, the peak power of the square pulse is about 1.04 W in the cavity, which is limited by the parameters of the mode-locked device [15], [16]. Here, the nonlinear gain saturation, large normal dispersion, and strong nonlinearity play key roles due to the 520-m ND-HNF used in the cavity.

The theory of DSR indicates that, when the parameters are chosen closer to the resonance point, the pulse energy could be enhanced to an infinitely large value and the pulse duration increases linearly with the pump power, whereas the pulse amplitude converges to a given plateau value [17]. The experiment results demonstrate that the resonance features of the square pulse are in qualitatively good agreement with the theoretical prediction. It can be confirmed that the DSR phenomenon has been experimentally observed in figure-of-eight fiber laser with large net-normal dispersion. The DSR generated in this paper is different from the typical DSR. For the typical DSR, the optical spectrum exhibits a square profile, and the pulse energy is limited by the formation of multipulse under strong pump power [26], [27]. In our experiment, the fiber laser delivers a stable square profile pulse and has higher pulse energy without wave breaking. Consequently, the pulse energy can be further increased by optimizing the laser parameters and employing a higher pump power.

4. Conclusion

In conclusion, the DSR with high-energy pulse has been experimentally observed in a passively mode-locked erbium-doped figure-of-eight fiber laser by using NALM technique. The fiber laser with a 520-m ND-HNF in the cavity operates in normal dispersion regime. The output of the fiber laser has a square profile pulse with the repetition rate of 369.7 kHz. With the increase of the pump power, the square-pulse duration increases linearly from 23.9 ns to 363.9 ns, whereas the peak power maintains around 1.04 W. And the pulse energy reaches up to 379.2 nJ without wave breaking. Such a high-energy square-pulse fiber laser with low peak power could be used as an ideal seed pulse source in the high-power pulsed amplification systems.

References

- [1] K. Tamura, E. P. Ippen, H. A. Haus, and L. E. Nelson, "77-fs pulse generation from a stretched-pulse mode-locked all-fiber ring laser," *Opt. Lett.*, vol. 18, no. 13, pp. 1080–1082, Jul. 1993.
- [2] H. A. Haus, K. Tamura, L. E. Nelson, and E. P. Ippen, "Stretched-pulse additive pulse mode-locking in fiber ring lasers: Theory and experiment," *IEEE J. Quantum Electron.*, vol. 31, no. 3, pp. 591–598, Mar. 1995.

- [3] F. Ö. Ilday, F. W. Wise, and T. Sosnowski, "High-energy femtosecond stretched-pulse fiber laser with a nonlinear optical loop mirror," *Opt. Lett.*, vol. 27, no. 17, pp. 1531–1533, Sep. 2002.
- [4] F. Ö. Ilday, J. R. Buckley, W. G. Clark, and F. W. Wise, "Self-similar evolution of parabolic pulses in a laser," *Phys. Rev. Lett.*, vol. 92, no. 21, pp. 213902-1–213902-4, May 2004.
- [5] J. R. Buckley, F. W. Wise, F. Ö. Ilday, and T. Sosnowski, "Femtosecond fiber lasers with pulse energies above 10 nJ," *Opt. Lett.*, vol. 30, no. 14, pp. 1888–1890, Jul. 2005.
- [6] A. Chong, J. Buckley, W. Renninger, and F. Wise, "All-normal-dispersion femtosecond fiber laser," *Opt. Exp.*, vol. 14, no. 21, pp. 10 095–10 100, Oct. 2006.
- [7] A. Chong, W. H. Renninger, and F. W. Wise, "All-normal-dispersion femtosecond fiber laser with pulse energy above 20 nJ," *Opt. Lett.*, vol. 32, no. 16, pp. 2408–2410, Aug. 2007.
- [8] F. W. Wise, A. Chong, and W. H. Renninger, "High-energy femtosecond fiber lasers based on pulse propagation at normal dispersion," *Laser Photon. Rev.*, vol. 2, no. 1/2, pp. 58–73, Feb. 2008.
- [9] L. M. Zhao, D. Y. Tang, T. H. Cheng, and C. Lu, "Nanosecond square pulse generation in fiber lasers with normal dispersion," *Opt. Commun.*, vol. 272, no. 2, pp. 431–434, Apr. 2007.
- [10] X. Liu, "Mechanism of high-energy pulse generation without wave breaking in mode-locked fiber lasers," *Phys. Rev. A*, vol. 82, no. 5, pp. 053808-1–053808-5, Nov. 2010.
- [11] D. J. Richardson, R. I. Laming, D. N. Payne, V. Matsas, and M. W. Phillips, "Selfstarting, passively modelocked erbium fibre ring laser based on the amplifying Sagnac switch," *Electron. Lett.*, vol. 27, no. 6, pp. 542–544, Mar. 1991.
- [12] D. Schmieder, P. L. Swart, and A. Booysen, "Figure-eight fibre lasers with NALM loops consisting of highly nonlinear dispersion shifted fibres for dense wavelength division multiplexing," in *Proc. IEEE AFRICON*, 2007, pp. 1–7.
- [13] V. J. Matsas, T. P. Newson, and M. N. Zervas, "Self-starting passively mode-locked fibre ring laser exploiting nonlinear polarisation switching," *Opt. Commun.*, vol. 92, no. 1–3, pp. 61–66, Aug. 1992.
- [14] N. Akhmediev, J. M. Soto-Crespo, and P. Grelu, "Roadmap to ultra-short record high-energy pulses out of laser oscillators," *Phys. Lett. A*, vol. 372, no. 17, pp. 3124–3128, Apr. 2008.
- [15] W. Chang, A. Ankiewicz, J. M. Soto-Crespo, and N. Akhmediev, "Dissipative soliton resonances," *Phys. Rev. A*, vol. 78, no. 2, pp. 023830-1–023830-9, Aug. 2008.
- [16] W. Chang, A. Ankiewicz, J. M. Soto-Crespo, and N. Akhmediev, "Dissipative soliton resonances in laser models with parameter management," *J. Opt. Soc. Amer. B*, vol. 25, no. 12, pp. 1972–1977, Dec. 2008.
- [17] P. Grelu, W. Chang, A. Ankiewicz, J. M. Soto-Crespo, and N. Akhmediev, "Dissipative soliton resonance as a guideline for high-energy pulse laser oscillators," *J. Opt. Soc. Amer. B*, vol. 27, no. 11, pp. 2336–2341, Nov. 2010.
- [18] W. Chang, J. M. Soto-Crespo, A. Ankiewicz, and N. Akhmediev, "Dissipative soliton resonances in the anomalous dispersion regime," *Phys. Rev. A*, vol. 79, no. 3, pp. 033840-1–033840-5, Mar. 2009.
- [19] X. Wu, D. Y. Tang, H. Zhang, and L. M. Zhao, "Dissipative soliton resonance in an all-normal-dispersion erbium-doped fiber laser," *Opt. Exp.*, vol. 17, no. 7, pp. 5580–5584, Mar. 2009.
- [20] L. Duan, X. Liu, D. Mao, L. Wang, and G. Wang, "Experimental observation of dissipative soliton resonance in an anomalous-dispersion fiber laser," *Opt. Exp.*, vol. 20, no. 1, pp. 265–270, Jan. 2012.
- [21] S. K. Wang, Q. Y. Ning, A. P. Luo, Z. B. Lin, Z. C. Luo, and W. C. Xu, "Dissipative soliton resonance in a passively mode-locked figure-eight fiber laser," *Opt. Exp.*, vol. 21, no. 2, pp. 2402–2407, Jan. 2013.
- [22] A. Cabasse, B. Ortaš, G. Martel, A. Hideur, and J. Limpert, "Dissipative solitons in a passively mode-locked Er-doped fiber with strong normal dispersion," *Opt. Exp.*, vol. 16, no. 23, pp. 19 322–19 329, Nov. 2008.
- [23] W. H. Renninger, A. Chong, and F. W. Wise, "Dissipative solitons in normal-dispersion fiber lasers," *Phys. Rev. A*, vol. 77, no. 2, pp. 023814-1–023814-4, Feb. 2008.
- [24] M. E. Fermann, F. Haberl, M. Hofer, and H. Hochreiter, "Nonlinear amplifying loop mirror," *Opt. Lett.*, vol. 15, no. 13, pp. 752–754, Jul. 1990.
- [25] C. B. Clausen, J. H. Povlsen, and K. Rottwitt, "Polarization sensitivity of the nonlinear amplifying loop mirror," *Opt. Lett.*, vol. 21, no. 19, pp. 1535–1537, Oct. 1996.
- [26] L. R. Wang, X. M. Liu, and Y. K. Gong, "Giant-chirp oscillator for ultra-large net-normal-dispersion fiber lasers," *Laser Phys. Lett.*, vol. 7, no. 1, pp. 63–67, Jan. 2010.
- [27] X. Liu, L. Wang, X. Li, H. Sun, A. Lin, K. Lu, Y. Wang, and W. Zhao, "Multistability evolution and hysteresis phenomena of dissipative solitons in a passively mode-locked fiber laser with large normal cavity dispersion," *Opt. Exp.*, vol. 17, no. 10, pp. 8506–8512, May 2009.